Numerical and Experimental Investigation of Zero-Gravity Distillation Units

Marc Wende, Florian Fischer, Eugeny Y. Kenig*

Chair of Fluid Process Engineering, Paderborn University, Pohlweg 55, 33098 Paderborn, Germany
eugeny.kenig@upb.de

Zero-gravity distillation (ZGD) represents an attractive method to perform small-scale distillation processes. In contrast to gravity in conventional distillation units, capillary forces, for example arising in metal foams, are used to guide the liquid phase. In this work, an experimental ZGD setup was constructed. A novel mathematical model was developed which allows the simulation of ZGD units. The model includes coupled momentum, heat and mass transfer equations for the liquid and vapor phases as well as heat conduction equation for the unit walls. The fluid dynamics is determined using the hydrodynamic analogy concept. The numerical simulations were successfully validated with the obtained experimental results.

1. Introduction

The use of small-scale modular equipment units has great potential in implementation of advanced energy and resource-efficient chemical plants. However, small-scale fluid separation equipment has not yet been developed far enough to be applied in production processes. This is particularly true for distillation, despite that this unit operation is one of the most important fluid separation methods for homogeneous liquid mixtures. A major reason for the slow technological progress in this area is the lack of necessary design fundamentals (Kenig et al., 2013).

Zero-gravity distillation (ZGD) suggests a way to establish a small-scale distillation process. Using the heat-pipe principle, a stable countercurrent flow of liquid and vapor phases can be realized. In contrast to conventional distillation units, capillary forces are exploited to ensure liquid flow in ZGD devices. Seok and Hwang (1981) published the first study on the distillation of methanol-water and ethanol-water mixtures. They used a tube with a wick made of fibreglass. The feed was supplied in the middle of the tube, and the product streams were withdrawn at the condenser and evaporator. The experiments were performed with and without total reflux. Seok and Hwang (1981) complemented their work with an analytical model based on Darcy's law for fluid flow and a species transport model based on experimentally determined mass transfer coefficients.

Ramirez-Gonzalez et al. (1992) presented a momentum transport model using the Young-Laplace equation and Darcy's law. Species transport was described by experimentally determined mass transfer coefficients, as in the work of Seok and Hwang (1981). An alternative approach was proposed by Tschernjaew et al. (1996). Here, again, the momentum transport was described by the Young-Laplace equation and Darcy's law. However, for species transfer, a model using the Maxwell-Stefan equations for multicomponent mixtures was applied. This model is largely independent of experimental data. The first approach to describe ZGD processes considering phase change phenomena was presented by Rieks et al. (2018) and further developed in (Rieks et al., 2019). They described the liquid and vapor phases using a hydrodynamic analogy based concept. An experimentally determined temperature profile was used as a thermal boundary condition at the heated/cooled wall.

Along with these theoretical works, a few experimental studies have been published. Preußer (2020) developed an experimental setup of a rectangular ZGD unit. A grooved structure was used as the porous material. Heat fluxes, temperature profiles and the fluid interface evolution were evaluated. Experimental studies with metal foams applied as porous structures were carried out by Sundberg et al. (2009). The proposed ZGD unit was, again, rectangular. In a later paper, Sundberg et al. (2013) developed a further ZGD column supplied with an evaporator and an external condenser.

The models presented above do not govern complete ZGD units and require experimentally determined parameters. Therefore, they are unable to predictively simulate ZGD units. To close this gap, in the present work, we developed a fully predictive model for ZGD with metal foams. This model describes both the transport phenomena in the vapor and liquid phases and the heat conduction in the walls.

Along with the modeling, experimental investigations of the ZGD unit were carried out. An experimental set-up similar to that presented by Sundberg et al. (2009) was built up, and the separation of an ethanol/water mixture was studied. The evaporation and condensation take place inside of the ZGD unit rather than in external heat exchangers. The feed and product streams are supplied to and withdrawn from the liquid phase of the unit. Experiments were carried out both in the total reflux mode and for an operation with feed and product streams, while the temperature and concentration profiles along the ZGD unit were recorded. The data obtained by measurements were used to validate the model.

2. Experimental setup

A rectangular shaped ZGD unit developed in this work is schematically shown in Figure 1. The casing is milled of aluminum and insulated from the environment. The unit has an internal length of 150 mm (x-direction) and a width of 50 mm (y-direction). The internal height is 20 mm (z-direction). The lengths of the evaporator zone and of the condenser zone are 50 mm. Inside the unit a metal foam is placed.
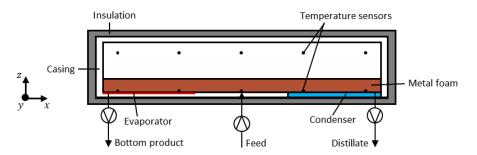

Figure 1: Schematic presentation of the experimental setup

Two different metal foams are used, both manufactured by Recemat International. The metal foams are highly porous, open-cell foams building an interconnected porous network. One metal foam is made of a nickel chromium alloy with a height h_M of 2 mm and a porosity ϵ of 0.93. The second metal foam is made of copper and has a height of 5 mm and a porosity of 0.95. For both metal foams, the effective pore diameter d_P is 0.6 mm. Temperature sensors are placed in the vapor and liquid phase to measure the relevant temperature profiles.

The heat is supplied to the evaporator by resistance heating cartridges. A thermostat is used to cool the condenser. The temperature of the water inside the thermostat can be set to a fixed value which affects the heat flow at the condenser.

Piston pumps are used to supply the feed and withdraw the distillate and bottom product from the liquid phase. In this work, the volume flow of the feed $\dot{F}$ is set to 1 ml/min. Samples of the liquid phase are taken from the sampling points. This allows the composition of the mixture to be determined between the feed and the product streams.

3. Mathematical model

A mathematical model of a ZGD unit is based in accordance with the experimental setup shown in Figure 1. The unit is filled with a vapor-liquid binary system. The liquid phase is embedded in the porous structure and covered by the vapor phase. At the condenser and evaporator, the corresponding distillate stream $\dot{D}$ and the bottom product stream $\dot{B}$ are withdrawn. The heat fluxes for the evaporator $\dot{q}_E$ and condenser $\dot{q}_C$ are considered at the lower wall. The ZGD unit is modeled in a two-dimensional approximation in the xz-plane. The corresponding computational domain with its boundary conditions is shown in Figure 2.

The fluid dynamics is described using the concept of hydrodynamic analogy (HA). The idea of this concept is to replace the actual process fluid flow by a simplified flow pattern or a combination of different simplified flow patterns (Kenig, 1997). If such an analogy is adequate, a rigorous description of heat and mass transport becomes possible. HA-models have already been successfully applied to describe different separation processes (see, e.g. Salten et al., 2018).

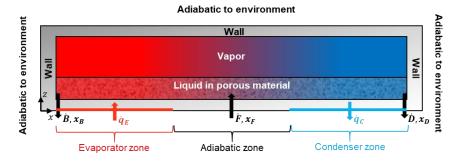In the present work, the capillary forces are assumed to be strong enough to immediately compensate for the

Figure 2: Sketch of the computational domain of the ZGD unit and its boundary conditions

movement of the liquid-vapor interface. As a result, it can be assumed that the phase interface coincides with the boundary between the porous structure and the vapor phase, as shown in Figure 2. The vapor-phase flow is considered in a simplified way as a creeping flow parallel to the liquid-vapor interface. Furthermore, the flow is steady and laminar. Under such conditions, the Navier-Stokes equation reduces to the following form:

$$\frac{\partial^2 u_v}{\partial z^2} = \frac{1}{\mu_v} \cdot \frac{\partial p_v}{\partial x} \tag{1}$$

Here u_v denotes the vapor-phase velocity, p_v is the pressure of the vapor phase and μ_v is its viscosity. As the boundary conditions for Eq(1) the no-slip condition at the upper wall and zero vapor velocity at the phase interface are applied. The liquid flow inside the metal foam is described by Darcy's law (Nield and Bejan, 1999):

$$-u_l = \frac{K}{\mu_l} \cdot \frac{\partial p_l}{\partial x} \tag{2}$$

where u_l is the liquid-phase velocity, μ_l is the liquid viscosity and K is the permeability, an empirical parameter depending on the structure of the metal foam.
A steady-state two-field formulation is used to describe the heat transport:

$$\rho_v u_v c_{p,v} \frac{\partial T_v}{\partial x} - \lambda_v \nabla^2 T_v = 0 \tag{3}$$

$$\rho_l u_l c_{p,l} \frac{\partial T_l}{\partial x} - \lambda_{l,eff} \nabla^2 T_l = 0 \tag{4}$$

where T_k is the temperature, ρ_k is the density and $c_{p,k}$ is the specific heat capacity for each phase, $k = \{l, v\}$. The thermal conductivity in the vapor phase is denoted as λ_v. The effective thermal conductivity $\lambda_{l,eff}$ in the liquid-solid region depends on the properties of the metal foam. An experimentally validated correlation for the effective thermal conductivity can be found in Bhattacharya et al. (2002). At the liquid-vapor interface, the thermodynamic equilibrium condition has to be fulfilled.
Within the walls of the ZGD apparatus, only heat conduction takes place. Subsequently, the transport equation for the wall is written as:

$$-\lambda_w \nabla^2 T_w = 0 \tag{5}$$

where λ_w is the thermal conductivity of the wall material. At all unit walls, the continuity condition for the heat fluxes normal to the wall surface has to be fulfilled.
The species transport is described by a steady-state, two-field formulation:

$$\rho_v u_v \frac{\partial c_v}{\partial x} - D_v \nabla^2 c_v = 0 \tag{6}$$

$$\rho_l u_l \frac{\partial c_l}{\partial x} - D_{l,eff} \nabla^2 c_l = 0 \tag{7}$$

Here, D_v and $D_{l,eff}$ are the effective diffusivities and c_v and c_l the concentrations of the light boiling component in the liquid and vapor phase, respectively. Thermodynamic equilibrium relationship serves as a boundary condition at the liquid-vapor phase interface. The walls are impermeable and zero-gradient boundary condition

is applied at the boundaries between the fluid phases and the walls. The effective diffusivity within the liquid-solid region is determined based on the diffusivity of the liquid phase D_l as follows (Weissberg, 1963):

$$D_{l,eff} = \epsilon D_l \tag{8}$$

The pressure in the vapor phase is obtained as a sum of the partial pressure p_i and p_j of individual species:

$$p_v(x) = p_i(x) + p_j(x) \tag{9}$$

It is assumed that the pressure remains constant over the cross-section. The pressure drop of the liquid inside the metal foam is calculated by Eq(2). The liquid-side total pressure drop is determined by the capillary pressure difference described by the Young-Laplace equation:

$$p_v - p_l = \frac{4\sigma \cos(\theta)}{d_P} \tag{10}$$

Here, σ is the surface tension, θ the contact angle and d_P the effective pore diameter. Furthermore, total mass flow rates in the vapor phase $\dot{G}$ and liquid phase $\dot{L}$ are obtained by balancing the local interfacial mass fluxes $\dot{m}$ at an arbitrary x-position:

$$\frac{d\dot{G}}{dx} = \dot{m} \cdot b \tag{11}$$

$$\frac{d\dot{L}}{dx} = -\dot{m} \cdot b \tag{12}$$

where b is the internal width (without walls) of the ZGD unit. The feed, bottom product and distillate streams are considered in the mass balance at the specific x-positions x_F, x_B, x_D where the streams are supplied to or removed from the unit (see Figure 2).

The mathematical model was implemented in the MATLAB® software. All equations were discretized with the finite difference method and solved sequentially and iteratively.

4. Results and Discussion

The distillation process of ethanol/water mixture at a pressure of 1 bar was investigated. The initial concentration of ethanol $x_{EtOH,0}$ was 0.4. The experimental parameters given in Section 2 and the pure component properties were used in the simulations. Fluid properties were taken from Linstrom and Mallard (2016). Diffusivities and equilibrium data were determined using methods described by Poling et al. (2001).

Figure 3 shows the results obtained for the ZGD with the nickel chromium alloy metal foam under total reflux. In Figure 3a, the experimental and simulated concentration profiles of ethanol in the liquid phase are presented. The ethanol mole fraction profile reveals that this light boiling component is accumulated at the condenser side; accordingly, water is accumulated at the opposite side of the unit. At the condenser, an ethanol mole fraction of 0.61 is obtained; at the evaporator it is equal to 0.2. A comparison between the numerical and experimental values shows a good agreement, with deviations below 10 %. Figure 3b shows the experimentally and
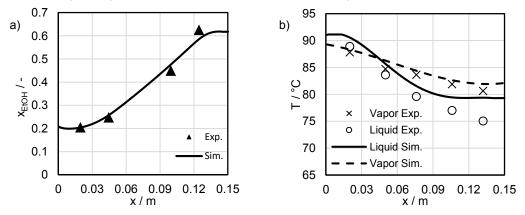

Figure 3: Results for ZGD with nickel chromium metal foam under total reflux: Experimentally and numerically determined ethanol mole fractions of ethanol in the liquid phase (a); Experimentally and numerically determined temperature *profiles (b).*

numerically determined temperature profiles of the liquid and vapor phases. Here, again, the simulated values fit the experimentally obtained quite well, while the maximum deviation is less than 7 %.

In Figure 4, the results for the ZGD with the copper metal foam under total reflux are depicted. The numerical and experimentally determined concentration profiles of ethanol in the liquid phase are presented in Figure 4a. Also, for this foam, the numerical results are in good agreement with experiments, showing deviations of less than 12%. The ethanol mole fraction at the condenser is 0.72, while at the evaporator, it is 0.14. Compared to the case with the nickel chromium metal foam, a higher separation efficiency is achieved. Our preliminary studies show that this effect is due to the higher thermal conductivity of copper rather than due to the difference in the metal foam height. Materials with high thermal conductivity appear to be beneficial for porous layer. In Figure 4b, the experimentally and numerically obtained temperature profiles are shown. Again, the simulated and experimental values are in good agreement, with a maximum deviation of 7.5 %.
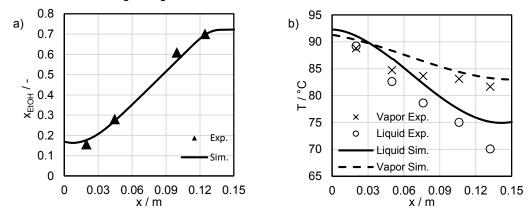

Figure 4: Results for ZGD with copper metal foam under total reflux: Experimentally and numerically determined mole fractions of ethanol in the liquid phase (a); Experimentally and numerically determined temperature profiles (b).

The results for the ZGD unit with feed and product streams are shown in Figure 5. As a porous structure, the copper metal foam was chosen. The ethanol mole fraction in the feed is 0.4. In Figure 5a, the experimentally and numerically determined ethanol concentration profiles are depicted. Also, for this mode, numerical and experimental values agree well, with the maximum deviation below 16 %. In the distillate stream, an ethanol mole fraction of 0.63 is achieved. The mole fraction in the bottom product stream is 0.13. Figure 5b presents the experimentally and numerically obtained temperature profiles, which, again, are close to each other, showing deviations of less than 6 %.
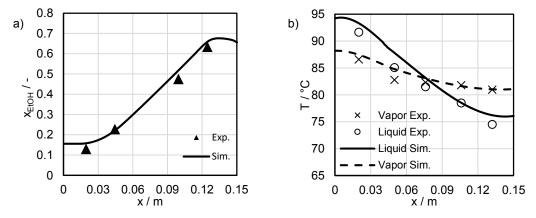

Figure 5: Results for ZGD copper metal foam and with feed and product streams: Experimentally and numerically determined mole fractions of ethanol in the liquid phase (a); Experimentally and numerically determined temperature profiles (b).

It is obvious that the obtained ethanol mole fraction at the condenser is lower than in the case of the ZGD with copper metal foam and total reflux. This is an expected result, which corresponds to the behavior of large-scale distillation units.

To compare the efficiency of the ZGD unit to that of large-scale distillation units, the method of the height equivalent to a theoretical plate ($HETP$) is used. In all three cases investigated in this work, the $HETP$-values are around 3.75 cm to 5 cm. These values show that the studied separation process is quite efficient. The $HETP$-values for a Mellapak 250.X are specified in a range between 45 and 70 cm.

It is worth noting that in all three cases, the temperature of the liquid phase at the evaporator is higher than in the vapor phase. This can be explained by the position of the evaporator. In contrast to the conventional distillation units, the heat is supplied to the unit directly through the bottom wall. At the same time, the high surface-to-volume ratio results in a stronger heat release of the vapor phase towards the walls.

5. Conclusions

In this work, an experimental setup for the ZGD investigation was built. The ZGD unit is able to operate both under total reflux and with feed and product streams. Two different metal foams were used as porous structures. The measurements were supplemented with a mathematical model based on the hydrodynamic analogy concept. It was found that the copper metal foam achieves a higher separation efficiency than the foam made of nickel chromium alloy. The separation efficiency decreases in the case of the ZGD with feed and product streams compared to the ZGD under total reflux. This is in line with the conventional behavior of large-scale distillation units. The experimentally and numerically obtained values of the ethanol mole fraction and the temperature profiles show a good agreement, with deviations below 16%. The mathematical model is successfully validated for both investigated operational modes. Furthermore, the studied ZGD units can be evaluated as more efficient than conventional large-scale distillation columns, with the HETP-values between 3.75 cm to 5 cm.

As the next steps, investigations of ZGD of different binary mixtures and with different unit dimensions are planned.

References

Bhattacharya, A., Calmidi, V.V., Mahajan, R.L., 2002. Thermophysical properties of high porosity metal foams. Int. J. Heat Mass Transfer 45, 1017–1031.

Kenig, E.Y., 1997. Multicomponent multiphase film-like systems: a modelling approach. Comput. Chem. Eng. 21 (supplement), 355–360.

Kenig, E.Y., Su, Y., Lautenschleger, A., Chasanis, P., Grünewald, M., 2013. Micro-separation of fluid systems: a state-of-the-art review. Sep. Purif. Technol. 120, 245–264.

Linstrom, P.J., Mallard, W.G., 2021. NIST Chemistry WebBook. NIST Standard Reference Database Number 69. National Institute of Standards and Technology, Gaithersburg MD, 2089.

Nield, D.A., Bejan, A., 1999. Convection in Porous Media. Springer, New York, USA.

Poling B.E., Prausnitz J.M., O'Connell J., 2001. The Properties of Gases and Liquids. McGraw-Hill, New York, USA

Preußer, N., 2020. Coupled Transport Processes in Zero-Gravity Distillation Columns. PhD Thesis. Technische Universität Darmstadt, Darmstadt, Germany.

Ramirez-Gonzalez, E.A., Martinez, C., Alvarez, J., 1992. Modeling zero-gravity distillation. Ind. Eng. Chem. Res. 31, 901–908.

Rieks, S., Preußer, N., Gambaryan-Roisman, T., Kenig, E.Y., 2018, Zero-gravity distillation with metal foams: A modelling approach, Chemical Engineering Transactions, 69, 283-288.

Rieks, S., Wende, M., Preußer, N., Gambaryan-Roisman, T., Kenig, E.Y., 2019. A hydrodynamic analogy based modelling approach for zero-gravity distillation with metal foams. Chem. Eng. Res. Des. 147, 615-623.

Salten, A.H.J., Mackowiak, J.F., Mackowiak, J., Kenig, E.Y., 2018. A novel approach to the modelling of transport phenomena in random packings. Chem. Eng. Trans. 69, 349-354.

Seok, D.R., Hwang, S.-T., 1985. Zero-gravity distillation utilizing the heat pipe principle (micro-distillation). AIChE J. 31, 2059–2065.

Sundberg, A., Uusi-Kyyny, P., Alopaeus, V., 2009. Novel micro-distillation column for process development. Chem. Eng. Res. Des. 87, 705-710.

Sundberg, A., Uusi-Kyyny, P., Jakobsson, K., Alopaeus, V., 2013. Control of reflux and reboil flow rates for milli and micro distillation. Chem. Eng. Res. Des. 91, 753-760.

Sulzer Chemtech Ltd., 2021. Structured Packings: Energy-efficient, innovative and profitable. <www.sulzer.com/en/shared/products/mellapak-and-mellapakplus> accessed 10/06/2021

Tschernjaew, J., Kenig, E.Y., Górak, A., 1996. Mikrodestillation von Mehrkomponentensystemen. Chem. Ing. Tech. 68, 272–276.

Weissberg, H., 1963. Effective diffusion coefficient in porous media. J. Appl. Phys. 34, 2636-2639.